Chinese Chemical Letters 34 (2023) 108053

Contents lists available at ScienceDirect

Chinese Chemical Letters

journal homepage: www.elsevier.com/locate/cclet

Single-particle detection of cholesterol based on the host-guest recognition induced plasmon resonance energy transfer

Shu-Min Wang[a], Hui Wang[a], Wei Zhao[a,b,*], Jing-Juan Xu[a,*], Hong-Yuan Chen[a]

[a] State Key Laboratory of Analytical Chemistry for Life Science, School of Chemistry and Chemical Engineering, Nanjing University, Nanjing 210023, China
[b] Institute of Nanochemistry and Nanobiology, School of Environmental and Chemical Engineering, Shanghai University, Shanghai 200444, China

ARTICLE INFO

Article history:
Received 30 June 2022
Revised 15 November 2022
Accepted 6 December 2022
Available online 9 December 2022

Keywords:
Dark field microscopy
Localized surface plasmon resonance
Plasmon resonance energy transfer
GNPs@CD nanoparticles
Cholesterol

ABSTRACT

Plasmon resonance energy transfer (PRET) occurs between the plasmonic nanoparticles (NPs) and organic dyes forming donor-acceptor pairs, which has great potential in quantitative analytical chemistry because of its excellent sensitivity under dark-field microscopy (DFM). Herein, we introduce supramolecular β-cyclodextrin (β-CD) to design a host-guest recognition plasmonic nano-structure modified gold nanoparticles (GNPs), while GNPs and rhodamine molecule (RB) act as the donor and acceptor, respectively. In the presence of the target cholesterol, due to the stronger binding of cholesterol with β-CD, RB molecules are released, inducing the inhibition of PRET, as well as the increase of the scattering intensity of GNPs. The proposed strategy achieves a linear range from 0.02 μmol/L to 2.0 μmol/L for cholesterol detection, and reaches a limit of detection (LOD) of 6.7 nmol/L. This host-guest recognition strategy can easily integrate receptor-donor pair into one nanoparticle, which simplifies the construction of the PRET platform, and further provides an effective approach for PRET-based analytical applications. Afterwards, the proposed PRET strategy was successfully applied for the detection of cholesterol in serum samples with high sensitivity and specificity. The proposed method provides an effective clinically potential means for the detection of cholesterol and other disease-related biomarkers.

Cholesterol is not only an essential component of animal cell membranes, but also the main precursor for the synthesis of different biomolecules such as bile acids, steroid hormones and vitamin D, and the only precursor of all steroid hormones [1–4]. The abnormal level of cholesterol in human serum would cause a variety of related dangerous diseases [5,6]. The total cholesterol count in human serum is one of the most important indexes in clinical diagnosis. Currently, a wide range of methods for the detection of cholesterol have been developed, such as electrochemistry [7], chromatography [8], enzyme-linked immunosorbent assay (ELISA) and fluorometry [2,9]. So far, the main clinical method for the detection of cholesterol is the ultraviolet-visible spectrophotometry based on the principle of photoelectric colorimetry. However, it suffers from problems of relatively high sample consumption and long time-consuming. Thus, it is in urgent need to construct cost-effective and time-saving strategy with high sensitivity and specificity.

Noble metal nanoparticles (NPs) exhibit excellent optical performances due to their unique localized surface plasmon resonance (LSPR) properties, which have attracted increasing attention and been gradually applied in the field of analytical chemistry. The LSPR properties of noble metal NPs depend on their composition, size, shape and surrounding medium environment. The adsorption and chemical reaction of small organic molecules and biological macromolecules can cause changes in the surface medium environments of noble metal NPs, which further influences the wavelength and intensity of their LSPR scattering spectra. In the early stage of LSPR absorption based sensing, a large number of NPs in the bulk solution were used for the quantitative analysis. In recent years, dark-field microscopy (DFM) provides the possibility of single-particle plasmonic imaging analysis. Single-particle plasmonic imaging not only significantly improves the sensitivity of the analytical detection [10–12], but also greatly reduces the sample consumption. Recently, a new form of energy transfer-plasmon resonance energy transfer (PRET) was proposed based on the LSPR properties of noble NPs. Technically speaking, PRET is Rayleigh scattering resonance energy transfer, which can be monitored by DFM imaging with great sensitivity and signal-to-noise ratio [13–15]. PRET is considered to be the non-radiative energy transfer process between plasmonic donor and resonant acceptor molecules through dipole-dipole interaction [16,17]. In 2007, Lee

* Corresponding authors.
E-mail addresses: wei_zhao@shu.edu.cn (W. Zhao), xujj@nju.edu.cn (J.-J. Xu).

https://doi.org/10.1016/j.cclet.2022.108053
1001-8417/

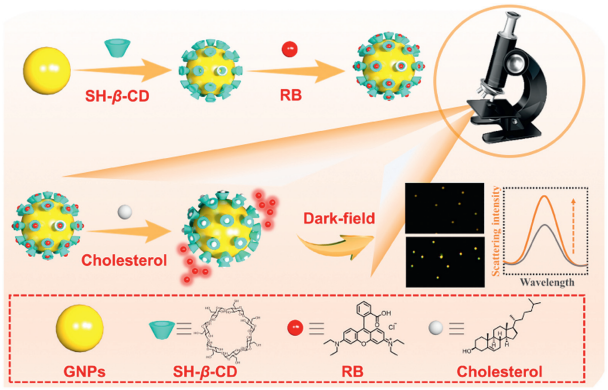

Scheme 1. Schematic illustration of single-particle detection of cholesterol.

and colleagues discovered that cytochrome C can induce the PRET phenomenon with GNPs and resulting in the changes of scattering spectrum [18]. Due to its high sensitivity and mature application, PRET effect based DFM single-particle imaging was widely used in various analytical chemistry fields, such as ion detection, biological imaging, and enzyme analysis [19–21]. At present, the challenge of PRET is to construct the suitable donor-acceptor pairs due to the lack of apposite energy acceptor chromophores and the additional complicated operation requirements for the connection with GNPs.

In this work, we constructed the detection platform of cholesterol based on the β-cyclodextrin (β-CD) modified GNPs (GNPs@CD NPs). β-CD is a macrocyclic compound composed of seven glucose units [22,23]. It has a hollow cone structure with lipophilic cavity and hydrophilic outer surface, which can be used as a multifunctional body and form host-guest inclusion compounds with thousand kinds of lipophilic guest molecules [24]. β-CD molecules exhibited different binding abilities toward various types of aromatic molecules (such as many dye fluorescent molecules), and have been widely applied in the field of catalysis, separation, drug loading and sensing, *etc*. The acceptor molecules in PRET systems are commonly dye fluorescent molecules with hydrophobic group, therefore, it is reasonable to introduce CD molecules for the construction of PRET platform. Considering the unique topological structure of β-CD molecules, their interaction with GNPs may significantly adjust the surface chemistry of GNPs and generate new properties and corresponding potential applications [25–28]. The introduction of β-CD molecules on the surface of GNPs simplified the additional complex connection requirements of GNPs, making it easier to construct donor-acceptor pairs. The distance between the donor and acceptor must be shorter than 1 nm, which contributes to the high quenching efficiency of the scattering signal. On this account, in virtue of the host-guest interaction between β-CD and cholesterol, a highly sensitive, specific and efficient detection method of cholesterol was established. The specific principle of this experiment is described in Scheme 1. As a commonly used fluorescent organic molecule, rhodamine molecule (RB) is preloaded into the cavity of β-CD. The position of the ultraviolet absorption spectrum of RB overlaps with the scattering spectrum of GNPs, making them an efficient donor-acceptor pair. On account of the generation of the PRET effect, the plasmon resonance energy of the donor GNPs is transferred to the acceptor molecule RB, resulting in the decrease of the scattering intensity of GNPs. The interaction energies of CD-cholesterol and CD-RB are -1.37 eV and -1.01 eV, respectively. A more negative energy value means higher stability of the resulting complexes. Therefore, cholesterol can effectively replace RB from the CD cavity [1,25]. While in the presence of cholesterol, the stronger host-guest binding ability of cholesterol with β-CD leads to the release of RB and preventing the occurrence of PRET, further the scatter signal

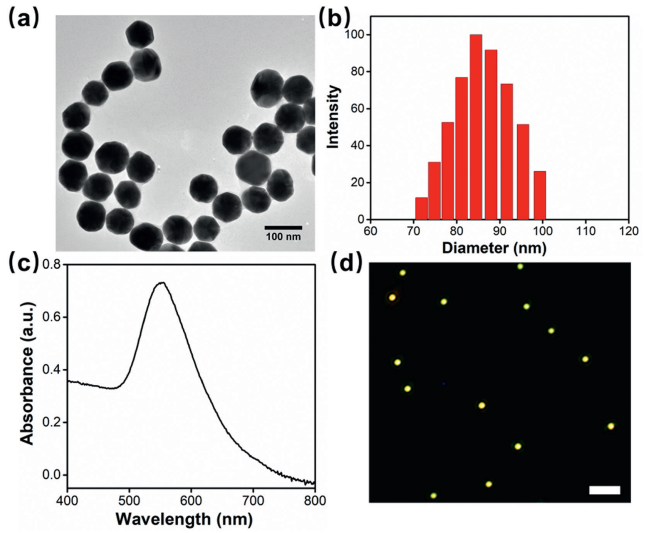

Fig. 1. (a) TEM, (b) Hydrodynamic size distribution and (c) UV–vis characterization of GNPs. (d) Representative DFM images of GNPs, scale bar: 5 μm.

of GNPs@CD gradually recovers. A linear dynamic range from 0.02 μmol/L to 2 μmol/L was achieved, with a limit of detection (LOD) down to 6.7 nmol/L. Overall, this PRET effect based platform provides a good opportunity for the clinical application of cholesterol sensing in human serum with high sensitivity and accuracy.

In this work, a straight, low-sample consumption and sensitive single particle plasmonic imaging approach for the detection of cholesterol was designed as illustrated in Scheme 1. In order to prepare GNPs with good morphology and uniformity, the seed-mediated growth method in the presence of sodium citrate and $HAuCl_4$ was introduced according to previous reports with some modification [29,30]. The synthesized GNPs show uniform morphology, which could be observed in the TEM image as shown in Fig. 1a. The size determined by statistical analysis is 73.2 ± 2.5 nm. And the dynamic light scattering (DLS) measurement of GNPs in Fig. 1b indicates that the particles possess a hydrated particle size of approximately 85 nm. In addition, the results of UV–vis absorption spectroscopy show that the prepared GNPs exhibit a characteristic resonance absorption peak at approximately 550 nm in Fig. 1c. It should be noticed that GNPs with diameter of 70–75 nm were considered as optimal observation objects under DFM, because they could be easily identified on single particle level and sensitive to the change of surrounding environments [31]. Most of the particles are bright kelly under DFM, further indicating that these GNPs have excellent uniformity and monodispersity (Fig. 1d).

As mentioned above, in order to establish the connection between β-CD and GNPs, SH-β-CD molecules were imported due to the strong Au-S bond. Briefly, GNPs@CD NPs were obtained by mixing 5 mL of prepared GNPs with 5 mL of SH-β-CD (10 mmol/L) aqueous solution. After reaction, the zeta potential changed from -39.7 ± 1.5 mV to -22.2 ± 1.8 mV, indicating the successful replacement of citrate by β-CD molecules. In addition, we also characterized GNPs@CD and β-CD molecules by Fourier transform infrared spectroscopy (FT-IR) respectively. As shown in Fig. S1 (Supporting information), the similarity of the two curves of the main characteristic groups of β-CD molecules further indicates the successful modification of β-CD molecules on GNPs. The supramolecular macrocycle on the surface of GNPs can be used as the scaffold of organic fluorophores, and the further formed host-guest composite NPs are expected to be used in the field of PRET based single-particle biosensing.

The strong overlap between the scattering spectra of GNPs and the absorption spectra of RB ensured the effective PRET. The UV–

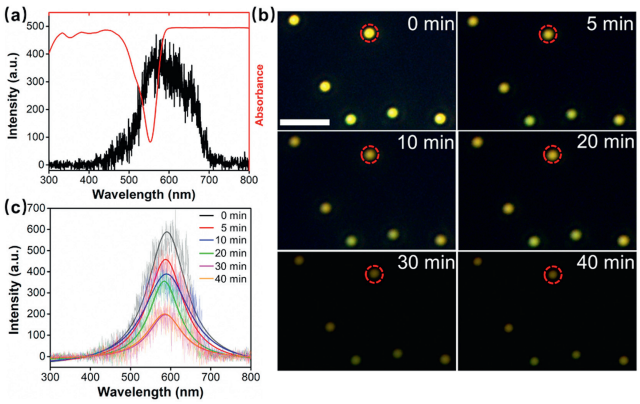

Fig. 2. (a) Spectral overlap between the plasmon resonance scattering of GNPs (black line) and the absorption of RB (red line). (b) Typical time-dependent DFM images (scale bar: 5 μm). (c) Corresponding scattering spectral changes of a single GNP (red circle) in (b) as a function of time.

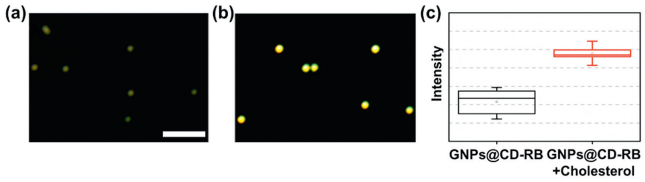

Fig. 3. DFM images of GNPs@CD-RB before (a) and after (b) exposure to cholesterol (scale bar: 5 μm). (c) Statistical analysis of gray values of particles in (a) and (b).

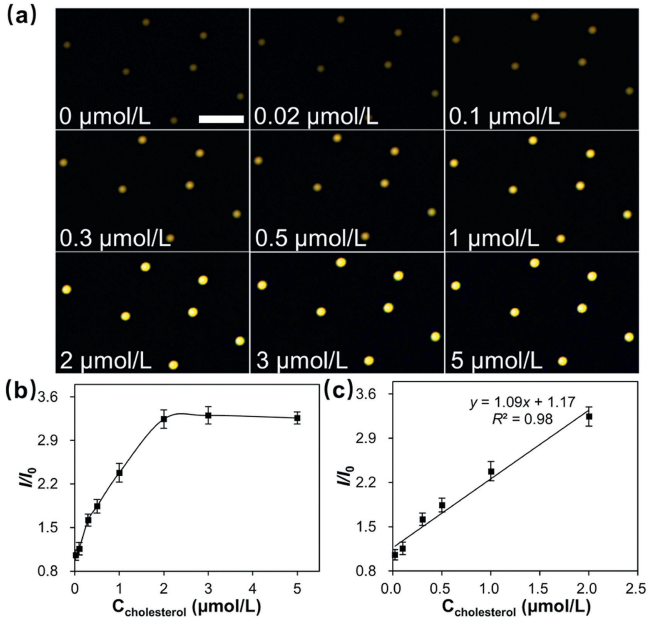

Fig. 4. (a) Representative DFM images of GNPs@CD-RB after adding different concentrations of cholesterol (0, 0.02, 0.1, 0.3, 0.5, 1, 2, 3, and 5 μmol/L, scale bar: 5 μm). (b) The relationship between the I/I_0 and the cholesterol. (c) Corresponding linear (from 0.02 μmol/L to 2 μmol/L) ranges of the determined ratio I/I_0.

vis absorption spectrum of RB in Fig. 2a shows with an absorption peak around 555 nm, which has a great overlap with the scattering spectrum of GNPs. Therefore, when RB molecules were introduced into the entire system, the host-guest recognition structure was formed between RB and GNPs@CD, leading to the occurrence of PRET effect and the gradually decrease in the scattering intensity of GNPs. In order to characterize the PRET process between GNPs and RB molecule, the in situ dark field imaging measurements were conducted. Specifically, the real-time monitoring of the reaction process is shown in Fig. 2b. In order to observe the process of host-guest recognition, a series of DFM images were acquired every few minutes in a randomly selected field of view. In the whole process, as the reaction time was prolonged, it is worth noting that the scattering intensity of the NPs gradually decreased, illustrating a complete formation of host-gust complex around the surface of GNPs. 40 min was chosen as the optimal time for follow-up DFM experiments. In addition, the corresponding scattering spectra of individual particles were also collected as shown in Fig. 2c, which displayed the similar variation trend with dark field images.

In order to explore the ability of GNPs@CD NPs to detect cholesterol, both dark field imaging and fluorescence detection were carried out. According to the standard deviations of the results, the reproducibility of the approach is good. As displayed in Figs. 3a and b, When the target cholesterol was introduced into the reaction system, β-CD and cholesterol had stronger binding ability than RB according to the higher binding constant, leading to the decrease in the efficiency of PRET. Subsequently, the scattering intensity of the nanoprobe gradually recovered under DFM, which verified the feasibility of this PRET based sensing system. The gray intensity values of the images collected before and after the reaction were statistically analyzed in Fig. 3c. The gray value as determined using by the software of ImageJ. Besides, the fluorescence of RB was quenched when inserted into the cavity of CD that modified on the surface of GNPs, while in the presence of cholesterol, due to the competitive effect between the guests, GNPs@CD NPs releases RB molecules and forms a host-guest complex with cholesterol, resulting in the restoration of the fluorescence of RB. As illustrated in Fig. S2a (Supporting information), as the increase of cholesterol concentration in the reaction system, GNPs@CD NPs gradually released RB molecules, and the fluorescence intensity of the reaction solution gradually recovered. Specifically, the relationship between the fluorescence intensity and cholesterol concentration is shown in Fig. S2b (Supporting information) through data analysis. The fluorescence spectra results were similar with the DFM measurements, which further proves the successful establishment of host guest recognition effect induced PRET biosensing system, which makes the measurement results more credible and universal.

The quantitative detection of cholesterol by the nanoprobe GNPs@CD-RB was carried out under DFM. Representative single-particle DFM images are shown in Fig. 4a. When the cholesterol concentration increased from 0.02 μmol/L to 5 μmol/L, the scattering intensity of particles gradually increased. The cholesterol can be accurately quantified according to the statistical analysis. In consideration of the errors between different batches of samples, relative ratios rather than absolute values are used in the quantitative analysis. Among them, I and I_0 are the gray values of the particles in the presence and absence of cholesterol, respectively. The relationship between the ratio and cholesterol concentration is shown in Figs. 4b and c. As the concentration increases gradually from 0.02 μmol/L to 5 μmol/L, the value of I/I_0 rises gradually and remains stable after reaching a plateau. In addition, it is found that the ratio I/I_0 has a good linear relationship with the cholesterol concentration from 0.02 μmol/L to 2 μmol/L, and the linear equation is $y = 1.09x + 1.17$ ($R^2 = 0.98$). The LOD (3σ) for cholesterol is calculated to be 6.7 nmol/L. Compared with quantitative analysis using a fluorescence spectrometer in the bulk solution, the single-particle plasmonic imaging using DFM can provide relatively higher sensitivity. These results suggest that the single particle plasmonic imaging method constructed by the supramolecular host-guest recognition can greatly improve the detection sensitivity, and it will be a promising single-particle level functional molecular detection biosensor.

Selectivity is a key feature to evaluate the applicability of the designed detection platform. Therefore, in order to evaluate the

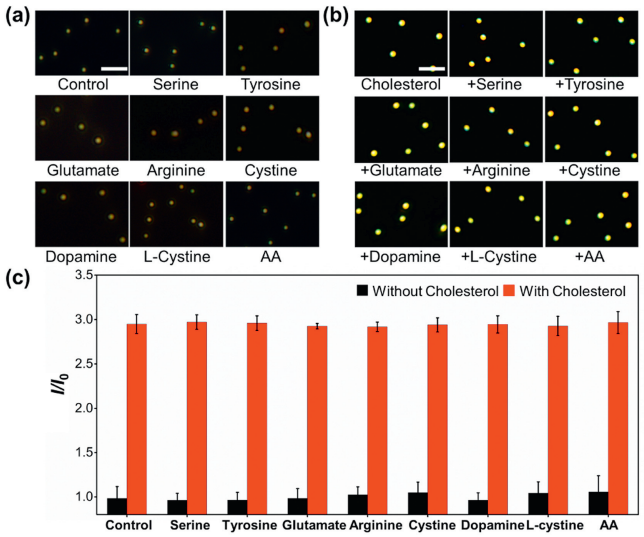

Fig. 5. (a) Typical DFM images of GNPs@CD NPs with various interfering substances in the absence of cholesterol. (b) Typical DFM images of GNPs@CD NPs in the presence of cholesterol and interfering substances, scale bar: 5 μm. (c) Column plots of ratio I/I_0 against the interference substances without and with cholesterol, respectively.

Table 1
Recovery estimations in human serum sample.

Samples	Spiked (μmol/L)	Detected (μmol/L)	Recovery (%)	RSD (%)
1	/	1.363	/	1.2
2	0.06	1.418	91.7	3.5
3	1.00	2.342	97.9	1.7
4	1.50	2.914	103.4	2.8

selectivity of this method for cholesterol, various interfering substances that may be present in biological samples, such as serine, tyrosine, glutamate, arginine, cystine, dopamine, L-cystine, and ascorbic acid (AA) (5 μmol/L) were then studied. Similarly, before the measurement of the solution at the single-particle level, we carried out the selectivity experiments at the single-particle level. These above-mentioned substances were added to the reaction solution instead of cholesterol. Representative DFM images of these reaction solutions are shown in Fig. 5a. Obviously, compared with the blank group, the scattering intensity of the particles remained almost unchanged. The calculated ratios I/I_0 of the nanoparticles are close to 1.0. However, when the mixture of cholesterol (2 μmol/L) and interfering substances (5 μmol/L) coexist, the scattering intensity of the nanoparticles is significantly enhanced (Fig. 5b), and the ratio reaches about 3. The above results all indicate that these substances do not interfere with cholesterol detection (Fig. 5c).

In order to prove the feasibility of this method in real biological samples, human serum samples were further used for testing. We used the standard addition method to evaluate the cholesterol level in the sample. Subsequently, a series of cholesterol concentrations (0, 0.06, 1.00, 1.50 μmol/L) were spiked into the diluted human serum, and cholesterol level was further determined through DFM imaging. The spiked recoveries between 91.7% and 103.4% were obtained with RSD from 1.2 to 3.5 as shown in Table 1, revealing the satisfactory accuracy of the proposed method for cholesterol detection in the diluted serum samples.

In conclusion, we have successfully constructed functionalized host-guest recognition plasmonic nanoprobe-GNPs@CD NPs, which is used to achieve sensitive and selective detection of cholesterol in human serum under DFM. By introducing supramolecular β-CD to form nanoparticles with a host-guest recognition structure, the plasmonic nanoprobe GNPs@CD NPs benefited from the effective PRET significantly overcomes the limitations of traditional colorimetry method. In the presence of cholesterol, due to its stronger binding ability with β-CD, the guest molecule RB that inserted into the CD cavity is released by competition, which inhibits PRET effect and further changes the scattering signals of GNPs. Through the statistical analysis of the data, sensitive and quantitative detection of cholesterol was realized. Benefited from the advantages of the constructed host-guest recognition plasmonic nanoparticles, we believe that the proposed biosensing strategy can provide important guidance for the development of PRET-based methods to analyze various disease biomarkers. The PRET approach shows strong universality and good potential for the clinical analysis.

Ethical statement

All of the serum samples were donated by patients in the First Affiliated Hospital of Nanjing Medical University. All of the investigation protocols in this study were approved by the Institutional Ethics Committees of Nanjing Medical University.

Declaration of competing interest

The authors declare that they have no known competing financial interests or personal relationships that could have appeared to influence the work reported in this paper.

Acknowledgments

This work was supported by the National Natural Science Foundation of China (Nos. 22034003 and 22074063), and Fundamental Research Funds for the Central Universities (No. 2022300285).

Supplementary materials

Supplementary material associated with this article can be found, in the online version, at doi:10.1016/j.cclet.2022.108053.

References

[1] J. Li, T. Liu, S. Liu, et al., Biosens. Bioelectron. 120 (2018) 137–143.
[2] H.C. Chang, J.A. Ho, Anal. Chem. 87 (2015) 10362–10367.
[3] P.W.F. Wilson, R.B. D'Agostino, D. Levy, et al., Circulation 97 (1998) 1837–1847.
[4] K. Simons, E. Ikonen, Science 290 (2000) 1721–1726.
[5] X. Jiang, Z. Tan, L. Lin, et al., Small Methods 2 (2018) 1800182.
[6] Q. Zhong, Z. Xie, H. Ding, et al., Small 11 (2015) 5766–5770.
[7] Y. Huang, J. Tan, L. Cui, et al., Biosens. Bioelectron. 102 (2018) 560–567.
[8] A. Sinha, S. Basiruddin, A. Chakraborty, et al., ACS Appl. Mater. Interfaces 7 (2015) 1340–1347.
[9] Q. Su, L. Gan, Y. Zhu, et al., Sens. Actuators B: Chem. 335 (2021) 129715.
[10] F. Qi, Y. Han, Z. Ye, et al., Anal. Chem. 90 (2018) 11146–11153.
[11] J. Ma, L. Zhan, R.S. Li, et al., Anal. Chem. 89 (2017) 8484–8489.
[12] S. Wang, Z. Ye, X. Wang, et al., ACS Appl. Nano Mater. 2 (2019) 6646–6654.
[13] T. Li, X. Xu, G. Zhang, et al., Anal. Chem. 88 (2016) 4188–4191.
[14] Z. Chen, J. Li, X. Chen, et al., J. Am. Chem. Soc. 137 (2015) 1903–1908.
[15] B. Xiong, Z. Huang, H. Zou, et al., ACS Nano 11 (2017) 541–548.
[16] J. Ma, M.X. Gao, H. Zuo, et al., Anal. Chem. 92 (2020) 14278–14283.
[17] P.F. Gao, Y.F. Li, C.Z. Huang, TrAC Trends Anal. Chem. 124 (2020) 115805.
[18] G.L. Liu, Y.T. Long, Y. Choi, et al., Nat. Methods 4 (2007) 1015–1017.
[19] Y. Cao, T. Xie, R.C. Qian, et al., Small 13 (2017) 1601955.
[20] X. Yan, C. Xia, B. Chen, et al., Anal. Chem. 92 (2020) 2130–2135.
[21] M.X. Gao, H.Y. Zou, Y.F. Li, et al., Anal. Chem. 89 (2017) 1808–1814.
[22] D. Wu, Y. Kong, Anal. Chem. 91 (2019) 5961–5967.
[23] Y. Wu, Z. Han, L. Wei, et al., Anal. Chem. 92 (2020) 5464–5472.
[24] D.M. Alzate-Sánchez, B.J. Smith, A. Alsbaiee, et al., Chem. Mater. 28 (2016) 8340–8346.
[25] Y. Zhao, Y. Huang, H. Zhu, et al., J. Am. Chem. Soc. 138 (2016) 16645–16654.
[26] D.N. Heo, W.K. Ko, H.J. Moon, et al., ACS Nano 8 (2014) 12049–12062.
[27] M. Koo, K.T. Oh, G. Noh, et al., ACS Appl. Mater. Interfaces 10 (2018) 24450–24458.
[28] Q. Ma, X. Fang, J. Zhang, et al., J. Mater. Chem. B 8 (2020) 4039–4045.
[29] Y. Wang, Y. Han, X. Tan, et al., J. Mater. Chem. B 9 (2021) 2584–2593.
[30] L. Xiao, L. Wei, X. Cheng, et al., Anal. Chem. 83 (2011) 7340–7347.
[31] H. Wang, C.H. Xu, W. Zhao, et al., Anal. Chem. 93 (2021) 10727–10734.